SSRG International Journal of Electrical and Electronics Engineering
ISSN: 2348-8379/ https://doi.org/10.14445/23488379/IJEEE-V13I11P111

Volume 13 Issue 11, 174-186, November 2026
© 2026 Seventh Sense Research Group®

Original Article

Design and Development of the UCH-SAT 3U Educational CubeSat: Computational Modeling of Enhanced EPS Management using Optimization Algorithms and Hybrid Energy Storage Systems (HESS)

Victor Romero-Alva[1], Jonathan Arzapalo-Torres[2], Raúl Gave-Barja[3]

[1,2]*Image Processing Research Laboratory (INTI-Lab), Universidad de Ciencias y Humanidades, Lima, Peru.*
[3]*Faculty of Engineering, Universidad Tecnológica del Perú, Peru.*

[1]*Corresponding Author : vromero@uch.edu.pe*

Received: 20 October 2026 Revised: 12 November 2026 Accepted: 17 November 2026 Published: 25 November 2026

Abstract - *This study developed UCH-SAT 3U, a modular educational CubeSat platform that integrates sensing, communication, onboard processing, image acquisition, actuation, and a basic power subsystem. A graphical interface was implemented to centralize the visualization of environmental variables, inertial orientation, subsystem status, camera acquisition, recording controls, and solar-panel deployment. As a complementary component, a computational model of the Electrical Power System (EPS) was developed to analyze photovoltaic generation, Maximum Power Point Tracking (MPPT), DC-bus dynamics, regulated outputs, and two energy-storage configurations. The photovoltaic model was tested between irradiance levels of 400 and 1000 W/m², with the MPPT algorithm offering tracking efficiency of 99.94% even in fluctuating irradiance. The battery-only system was able to reach a minimum DC-bus voltage of 14.122 V and maximum battery current of 1.831 A during load transients. With battery-supercapacitor hybrid, the minimum DC-bus voltage became 14.400 V, with the maximum battery current down to 0.946 A (48.3% decrease). With 3.3 V, 5V, and 12 V regulated outputs functioning properly, no violation occurred to any controller. Thus, it was concluded that UCH-SAT 3U system, including physical platform, graphical interface, and EPS computational model, represents various means of interaction and energy behavior analysis in education CubeSat.*

Keywords - *CubeSat, Electrical power system, Graphical User Interface, Maximum power point tracking, Supercapacitor.*

1. Introduction

The development of CubeSats has experienced considerable growth due to their standardized architecture, lower cost, and ability to carry out scientific, academic, and educational missions using small-scale platforms. By January 2024, more than 2,000 CubeSats had been launched into space worldwide [1].

Furthermore, through NASA's CubeSat Launch Initiative alone, approximately 150 CubeSats have been placed into orbit via more than 40 ELaNA missions, and more than 200 missions from over 100 organizations have been selected [2].

However, despite the increase in the number of missions, integration and system reliability issues persist. Studies of previous CubeSat generations indicated failure rates of around 40%, with integration, interface, and subsystem difficulties being the main problems [3]. Therefore, one of the main challenges remains reliably integrating communication, processing, sensing, and power functions while adhering to strict mass, volume, and power limitations.

Within the CubeSat subsystems, the Electrical Power System (EPS) plays a crucial role, as it is responsible for generating, storing, and supplying power to the other CubeSat components [6]. Problems associated with this subsystem can directly compromise mission operations. Reliability studies have estimated that between 26.76% and 41.06% of CubeSats may fail during their first year in orbit; furthermore, approximately 44% of failures occurring during the first 30 days are related to the power supply system [5].

Given these limitations, modeling and simulation offer an effective way to analyze energy behavior before the physical system is built. Models representing solar panels, batteries, and power control units have been developed to size components and study the behavior of the EPS under different operating conditions [4]. Thus, through simulation, it is possible to anticipate an energy architecture and thereby

This is an open access article under the CC BY-NC-ND license (http://creativecommons.org/licenses/by-nc-nd/4.0/)

reduce uncertainties before physical implementation. At the national level, there is a growing interest in developing capabilities related to small satellites and space technologies. In 2023, the Peruvian Space Agency (CONIDA) launched the project "CubeSats in Peru: From the Classroom to Space," which consisted of 16 team members and provided training to five students, one teacher, and three mentors. The first phase consisted of training, nanosatellite assembly, and the deployment of ground stations, and covered topics in space engineering, electronics, and programming [7].

At the university level, there are also initiatives such as Chasqui II at the National University of Engineering, which began with digital simulations and continued with the assembly and validation phase of the CubeSat; the project also demonstrated that funding, infrastructure, and specialized equipment were required to proceed with the implementation and pre-flight testing phases [8]. This reaffirms the importance of having accessible platforms that enable the development of design, integration, and simulation capabilities until higher levels of cost and complexity are reached.

In this regard, UCH-SAT 3U is being developed as a modular educational platform that integrates the various stages of a CubeSat system, ranging from the acquisition of data via sensors, communication between modules, processing by an onboard computer, image acquisition, and actuator mechanisms. Experience gained in the university setting shows that CubeSat projects allow students to engage in real-world activities involving the design, construction, integration, and operation of electronic systems [9]. The development of this type of platform requires ensuring the interaction of subsystems through systematic design, integration, and testing procedures [10]. In this paper, UCH-SAT serves as the physical integration platform, along with modeling and simulation of an EPS.

Based on this context, the literature review identified various proposals focused on the design, integration, and validation of CubeSat platforms. This background information made it possible to identify the main strategies used in the development of CubeSats. Significant progress was made, although gaps were also found in the understanding of the phenomenon, which made it necessary to analyze the most relevant studies in detail.

The design of educational CubeSat platforms relies on two important aspects: spatial efficiency and integration of subsystems. Bouwmeester et al. [11] suggest that the main functions of the platform should be integrated into the same unit in order to eliminate the need for numerous circuits as well as free up more space for experiments. In addition, Karkun [12] develops a modular architecture for its 3U CubeSat platform based on 6061-T6 aluminum and stacked electronic circuits, which makes it possible to organize the internal layout of the onboard computer, sensors, and components belonging to the power system. In both cases, the authors provide solutions designed to improve the use of available space and integration of elements of educational platforms.

Regarding communications, Abdullah et al. [13] formulate a modular architecture for 1U CubeSats built on a combination of a Zynq-7000 FPGA-based onboard computer and an S-band communications system that employs patch antennas and compact filters as an effective hardware solution and provides better quality of data transmission.

Meanwhile, Rastinasab and Weidong [14] devise a modular telemetry system based on a superheterodyne architecture and Arduino microcontroller split into reception, transmission, and filtering boards. The discussed ideas show different levels of complexity in communication implementation, varying from sophisticated systems to a modular architecture proposed for experimentation and diagnostics purposes.

Researchers have investigated Commercial off-the-Shelf (COTS) components for ease of academic platform development. An experimental CubeSat of the 1U type developed by Garcia-Fernandez et al. [15] has been designed based on an ATMEGA328P microcontroller, and it includes commercial sensors, wireless technology capable of buck-boost conversion and solar panels, thus merging physical variable acquisition with power management all in one system. Sethi et al. [16] have also applied COTS components for the development of power and communication subsystems with the utilization of MPPT technology as well as radio-frequency transceivers installed on the printed circuit boards. Both studies demonstrate that the use of commercial off-the-shelf components enables the implementation of functional architectures for experimentation and validation in university settings.

With regard to the electrical power system, Casado et al. [17] developed an EPS architecture that integrates triple-junction solar panels, buck regulators with MPPT control, and protected power distribution units, complementing the design with hardware-in-the-loop simulation techniques.

Similarly, Edpuganti and others [18] recognize the EPS as being one of the most important subsystems in the CubeSat structure since it is responsible for providing power to the OBC and communication systems, attitude control, and data handling systems. Moreover, the authors explain that it is also crucial to differentiate between the different operation modes in order to control the consumption of power according to the mission priorities.

The physical integration of other elements contributes to the effective utilization of the CubeSat's structure. According to Bakkali and colleagues, a triangular slot antenna is

integrated with the aluminum frame, using the frame as a reflector and minimizing the space taken up by the antenna itself. This allows for the maximization of the available surface area and results in freeing enough space for other systems, such as solar cells.

From the literature review, it is clear that Electrical Power System (EPS) is one of the vital and crucial subsystems of CubeSat, as it is the one on which all other subsystems rely upon. In this regard, the present study covers two lines of development at once. Firstly, the UCH-SAT 3U serves as an educational device intended to demonstrate how each step of a fully functioning communication, data sensing and processing system operates. On the other hand, the development of an EPS focused on efficient energy management.

The integration of both aims to establish a modular and functional educational platform, in which the UCH-SAT serves as an experimental environment, and the EPS can be evaluated under conditions representative of actual operation.

This research is structured as follows: Section 2 presents the methodology employed; Section 3 sets out the results obtained, along with the discussion; and finally, the study's conclusions are presented in Section 4.

2. Methodology

This research adopted a quantitative approach that was applied and focused on technological development. The Design Science Research Methodology (DSRM) was used as the methodological framework, which consists of six activities: problem identification and motivation, definition of solution objectives, design and development, demonstration, evaluation, and communication [20]. As shown in Figure 1.

The methodology was applied to the development and integration of the UCH-SAT 3U educational platform and to the design of a mathematical model of the Electric Power System (EPS). The energy model made it possible to analyze photovoltaic generation, maximum power point tracking, energy storage, bus regulation, and the system's response to different load conditions through computational integration.



Fig. 1 Design Science Research Methodology (DSRM)

2.1. Problem Identification and Motivation

The development of the UCH-SAT arose from the need for an educational platform that would demonstrate how different stages of electronic systems can be integrated into a more complex system, such as a CubeSat.

To this end, a Three-Unit (3U) structure was designed to integrate the acquisition of environmental and inertial variables, communication, processing via an onboard computer, image acquisition, actuation, and power supply.

At the same time, the need to analyze the energy behavior associated with the operation of these subsystems was identified. Because the physical platform has a basic power supply system, it was proposed to develop a mathematical model of an Electric Power System (EPS) that would allow for the study of photovoltaic generation, energy storage, regulation, and distribution.

The model was designed for integration with the Raspberry Pi 4, with the aim of complementing the physical platform by representing and analyzing its energy behavior.

2.2. Definition of the Solution Objectives

2.2.1. UCH-SAT 3U Requirements

The main requirements established for the UCH-SAT 3U educational platform were as follows:

- Integrate the three subsystems into a 3U structure.
- Acquire environmental and inertial variables via sensors.
- Enable communication between the various modules.
- Centralize processing using the On-Board Computer (OBC).
- Incorporate image acquisition and visual monitoring.
- Control the solar panel deployment mechanism.
- Enable monitoring of the system's overall operation.
- Maintain mechanical, electrical, and communication compatibility among the subsystems.

2.2.2. Electrical Power System (EPS) Computational Model Requirements

To complement the operation of the physical platform, the following requirements were established for the EPS mathematical-computational model:

- Model energy generation via photovoltaic panels.
- Incorporate Maximum Power Point Tracking (MPPT) using an MPPT algorithm.
- Model the dynamic behavior of the DC bus.
- Represent the regulated 3.3 V, 5 V, and 12 V outputs required by various loads.
- Enable the visualization of key energy-related variables.
- Allow for computational integration with the UCH-SAT's on-board computer.

2.3. Design and Development

2.3.1. UCH-SAT 3U Development and Architecture

As the first step in developing this project, UCH-SAT proposed an educational CubeSat with three subsystems (3U) for university academic use.

The integration of the following subsystems was considered: power supply, onboard computer with sensors, and communications.

Electronic and Functional Architecture

Based on the existing literature, the main challenges in CubeSat construction were identified as: available power capacity, physical dimensions, and payload. Due to these limitations, the components of the communications subsystem, including the antenna, must be designed to be as compact and lightweight as possible. The selected components are shown in Table 1.

Table 1. Main components and functions of the UCH-SAT 3U subsystems

	Components	Description
1	ESP32CAM	Image capture for visual monitoring and onboard observation
	AirTag Apple	Auxiliary tracking and prototype recovery
	NRF24L01	Radio-frequency wireless communication.
	MicroBit v2	Interactive module for system status indication and user feedback.
2	MQ-135	Air-quality and gas monitoring.
	MQ-131	Ozone detection
	MLX90614	Infrared temperature sensing.
	MS5611	Atmospheric pressure and altitude measurement
	Arduino Nano	Sensor acquisition and local data processing
	BME280	Temperature, pressure, and humidity sensing
	MPU6050	Motion and orientation measurement
3	Solar panels	Main electrical energy source
	CN3065	Solar LiPo battery charging
	LiPo	Energy storage and backup supply
	Arduino Nano	Dedicated power and actuator management
	MPU6050	Secondary IMU for backup, comparison, or dual sensing
	Servo Motors	Activation mechanism for the deployment of solar panels
OBC	Raspberry Pi 4	Main processing, telemetry, and system coordination

In addition, three subsystems covering the essentials were established, along with an onboard computer to process the data. As shown in Figure 2, the subsystems are:

- Communications subsystem (1)
- Sensing subsystem (2)
- Power subsystem (3)
- On-Board Computer (OBC)

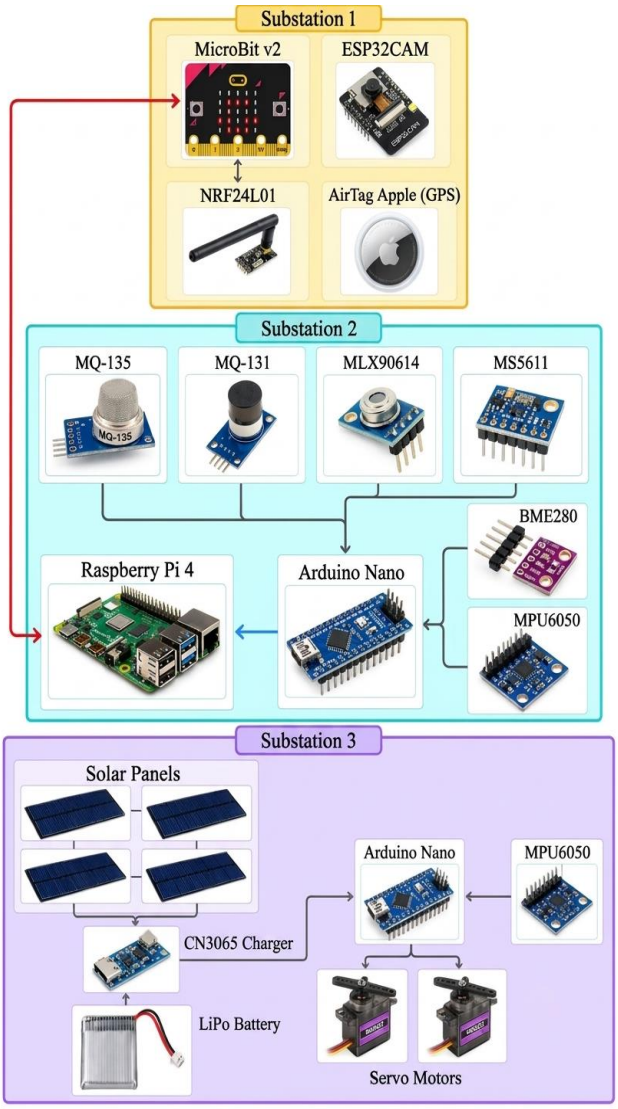

Fig. 2 Electronic architecture of the UCH-SAT subsystems as a whole

Next, the algorithm was developed (see Figure 3) to detect energy levels, with the goal of activating the solar panels and recharging itself. When the recharging process begins, the device enters a power-saving mode. In this state, it does not shut down completely, but minimizes energy consumption by deactivating various non-essential, high-power-consumption peripherals, thereby enabling faster recharging.

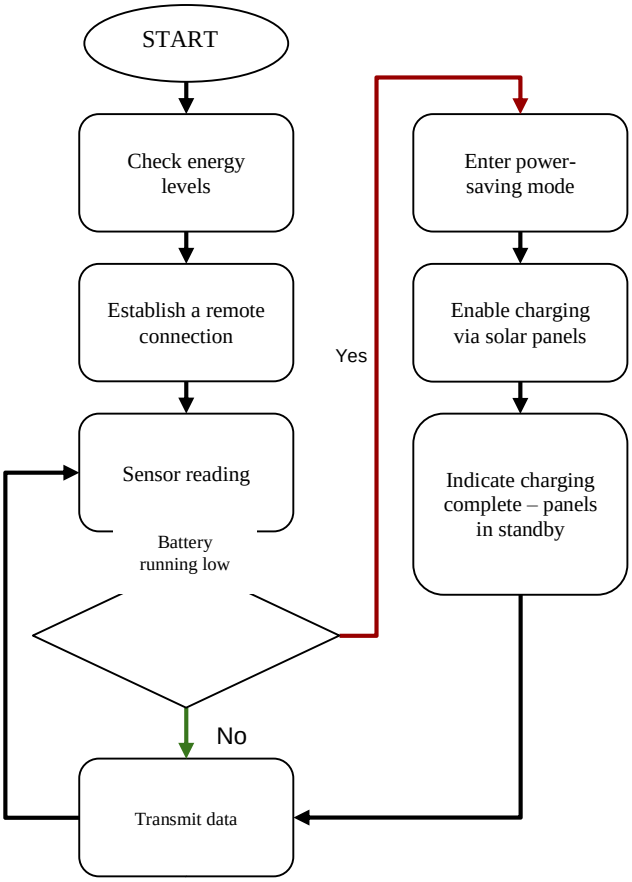

Fig. 3 UCH-SAT flowchart

Mechanical Architecture

For the mechanical design, a 2D drawing was created with top and side views, as shown in Figure 4. The substations have the same dimensions 10 cm x 10 cm x 10 cm and are connected by four supports.

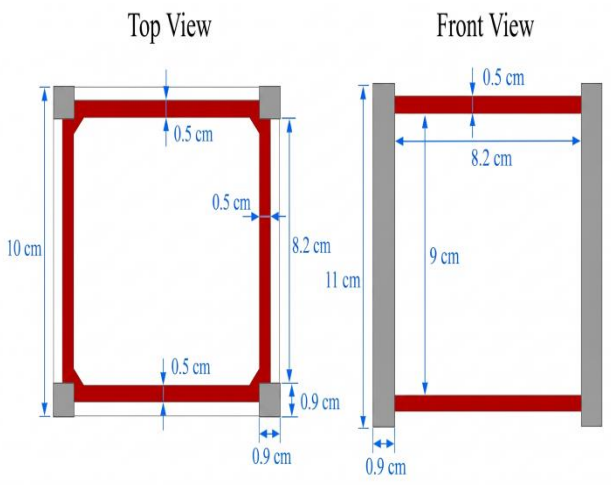

Fig. 4 Orthographic views and main dimensions of the UCH-SAT structure

Once the dimensions for each level were determined, a specific model was developed for each substation, based on the role it plays within the overall system, as shown in Figure 5.

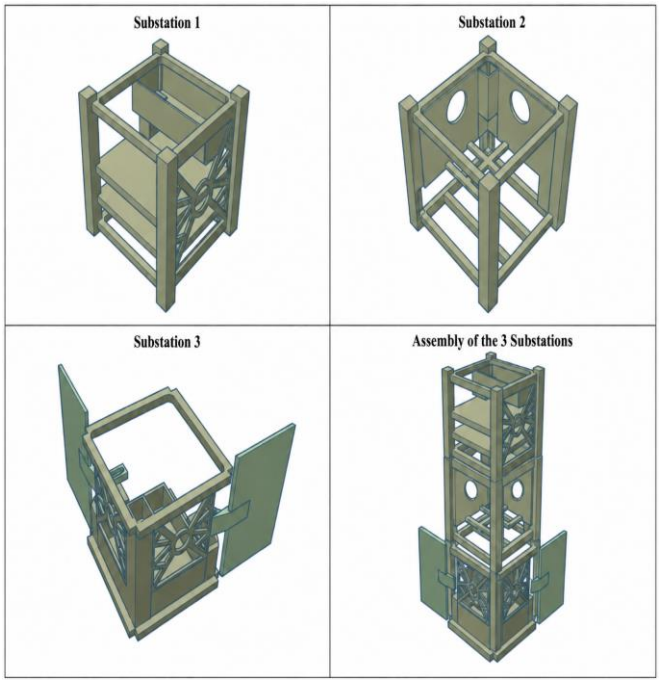

Fig. 5 Modular CAD design and assembly of the three UCH-SAT substations

First, the first substation houses the ESP32-CAM, so it includes a compartment that positions the camera facing upward. Additionally, platforms were integrated to accommodate the micro: bit, the MLX90614 temperature sensor, and an AirTag.

Second, the second substation was designed to accommodate the PCB and onboard computers, as well as specific openings for integrating the MQ-135 and MQ-131 sensors.

Finally, the third substation was designed with two movable fins driven by servomotors for the installation of solar panels, as well as a compartment for the servo control system and the battery charging module.

Subsystem Implementation and Interfaces

In order to view sensor data in real time, a Graphical User Interface (GUI) was designed in Figma with a well-organized layout. The graphical interface displays the panel openings, the orientation of the IMU sensor, atmospheric values from the sensors, and the option to view images and record data if necessary.

2.3.2. Electrical Power System Modeling and Computational Integration

To complement the UCH-SAT 3U physical platform, a mathematical-computational model of the Electric Power System (EPS) was developed to represent and enable the analysis of the main processes related to energy generation, storage, and distribution. Unlike the basic power supply system physically incorporated into the prototype, this model allowed for the study of energy variables under different generation conditions. This architecture consisted of a photovoltaic generation model, a Maximum Power Point Tracking (MPPT) algorithm, a DC bus, energy storage elements, and regulated outputs of 3.3 V, 5 V, and 12 V. This design made it possible to represent the energy flow from the generation source to the loads distributed across the various subsystems. The general architecture of the model is shown in Figure 6.

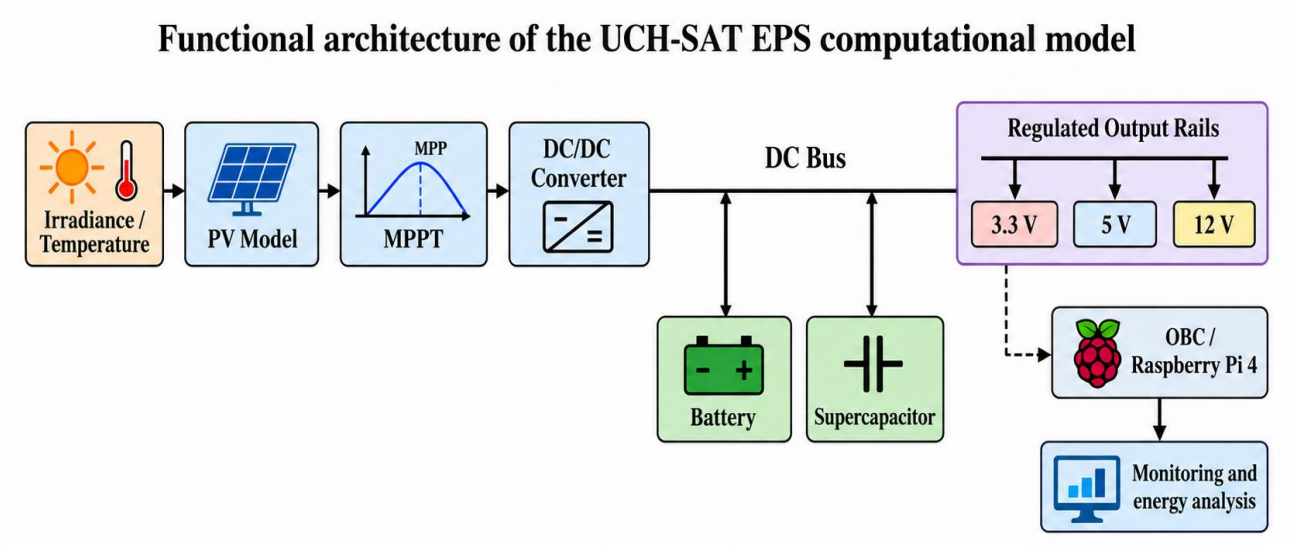

Fig. 6 Functional architecture of the UCH-SAT EPS computational model

Photovoltaic Model

The behavior of the photovoltaic array was represented using a single-diode equivalent model. The generated current was calculated as follows:

$$I_{PV} = I_{ph} - I_0 \left[exp\left(\frac{V_{PV}+I_{PV}R_s}{nN_sV_T}\right) - 1 \right] - \frac{V_{PV}+I_{PV}R_s}{R_{sh}}$$

Where I_{PV} it is the output current of the photovoltaic array, I_{ph} it is the photogenerated current, I_0 it is the diode's saturation current, V_{PV} it is the voltage of the array, R_s it is the equivalent series resistance, R_{sh} it is the equivalent parallel resistance, n it is the diode ideality factor, N_s is the number of cells connected in series, and V_T it is the thermal voltage.

The power generated instantaneously by the photovoltaic array is obtained by:

$$P_{PV} = V_{PV} I_{PV}$$

Where P_{PV} represents the electrical power generated by the photovoltaic array, V_{PV} the operating voltage e I_{PV} the corresponding current. Irradiance and temperature were considered as input variables for the model.

MPPT Model

To track the maximum power point, a Perturb-and-Observe (P&O) algorithm was implemented. In each calculation interval, the photovoltaic power was determined using:

$$P(k) = V(k)I(k)$$

Where P(k) corresponds to the photovoltaic power at the discrete instant k, V(k) is the panel voltage e I(k) it is the current generated at that very instant. Subsequently, the variations in power and voltage were calculated:

$$\Delta P = P(k) - P(k-1)$$

$$\Delta V = V(k) - V(k-1)$$

Where ΔP represents the change in power between two consecutive iterations and ΔV It represents the change in the photovoltaic voltage. Depending on the sign of the variations, the algorithm either maintains or reverses the perturbation applied to the operating point, with the goal of reaching the maximum power point.

Power Conversion and DC Bus

The DC-DC conversion stages were represented using average models. The DC bus was modeled based on the instantaneous power balance; therefore, an imbalance in generation, storage, or consumption should temporarily result in a change in one of its voltage levels:

$$\frac{dV_{bus}}{dt} = \frac{P_{net}}{C_{bus}V_{bus}}$$

Where V_{bus} it is the instantaneous bus voltage DC, C_{bus} is the equivalent capacitance associated with the bus, and P_{net} represents the net power; the latter was determined as follows:

$$P_{net} = P_{PV,bus} + P_{bat,bus} + P_{SC,bus} - P_{load,bus}$$

Where $P_{PV,bus}$ it is the power provided by the photovoltaic stage to the bus, $P_{bat,bus}$ is the power exchanged with the battery, $P_{SC,bus}$ is the power exchanged with the supercapacitor, and $P_{load,bus}$ It is the total power demanded by the loads.

Battery Model

Primary storage was represented by a rechargeable battery. For the dynamic analysis, an equivalent model consisting of an open-circuit voltage and an internal resistance was used:

$$V_{bat} = V_{OC} - I_{bat}R_{int}$$

Where V_{bat} It is the voltage available at the battery terminals, V_{OC} It is the open-circuit voltage, which depends on the state of charge, I_{bat} is the exchanged current, and R_{int} It is the equivalent internal resistance. The state of charge was updated internally during each simulation interval.

Supercapacitor Model

To study a hybrid storage configuration, a supercapacitor was incorporated, the relationship between its current and voltage variation being defined by:

$$I_{SC} = C_{SC}\frac{dV_{SC}}{dt}$$

Where I_{SC} it is the supercapacitor current, C_{SC} is its equivalent capacitance, and V_{SC} it is the stored voltage. This relationship made it possible to represent its contribution during rapid variations in demand.

Integration with the Onboard Computer

The Raspberry Pi 4 served as the integration point between the physical platform, data acquisition, and mathematical model simulation. In this way, the onboard computer complemented the UCH-SAT's processing and monitoring functions with information related to power, energy demand, and the behavior of the storage elements.

At the same time, the graphical user interface allowed for the centralized display of variables acquired by the sensors, the status of the subsystems, image acquisition, and information related to the platform's overall performance. Thus, UCH-SAT is not merely a collection of electronic circuits; it also features visual feedback to observe the

behavior of the subsystems and an energy model to analyze the behavior of the EPS under different operating conditions.

2.4. Demonstration

The demonstration included functional tests of the physical subsystems of the UCH-SAT 3U, covering the acquisition of environmental and inertial variables, communication between modules, processing by the onboard computer, image acquisition, and the actuation mechanisms associated with the solar panels. It also included verification of the display of key variables and statuses via the graphical interface.

In addition, the EPS model was run under different generation and demand conditions. To characterize the photovoltaic behavior, irradiance levels of 400, 600, 800, and 1000 W/m^2 were considered.

Subsequently, temporal variations in irradiance were applied to evaluate MPPT tracking, and transient load changes were applied to analyze the response of the DC bus and the storage elements. Finally, battery-only and hybrid configurations were evaluated.

2.5. Evaluation

The evaluation considered functional indicators for the physical platform and the graphical interface, as well as quantitative indicators for the energy model. On the UCH-SAT 3U, the operation of the sensing, communication, processing, image acquisition, and actuation subsystems was verified. For the graphical interface, the integrated display of the acquired variables and the main operating states was verified.

For the energy model, the following were analyzed: the response of the photovoltaic system, Maximum Power Point Tracking (MPPT), DC bus voltage, stability of the regulated outputs, and currents associated with the storage elements. The efficiency of the MPPT tracking was calculated using:

$$\eta_{MPPT} = \frac{\int_{t_0}^{t_f} P_{tracked}(t)dt}{\int_{t_0}^{t_f} P_{MPP,ref}(t)dt} \times 100$$

Where η_{MPPT} it is the tracking efficiency expressed as a percentage, $P_{tracked}(t)$ it is the power obtained by the algorithm MPPT, $P_{MPP,ref(t)}$ it is the maximum available power used as a reference, t_0 it is the initial moment and t_f It is the final instant of the evaluated interval.

To test the battery-only and hybrid configurations, the same load conditions were used, and the minimum DC bus voltage and the maximum current drawn from the battery were recorded.

2.6. Communication

The results obtained were documented by distinguishing between the behavior of the UCH-SAT 3U physical platform, the operation of the graphical interface, and the results generated by the energy model.

This distinction made it possible to differentiate between observations from tests conducted on the physical prototype and those obtained through the computational representation of the EPS.

Finally, the main findings and limitations of the development were analyzed, as well as the possibilities for improving the integration between the onboard computer, the graphical interface, and the energy model.

3. Results and Discussion

3.1. Results

3.1.1. UCH-SAT 3U Implementation and Functional Verification

The physical implementation of the UCH-SAT 3U made it possible to integrate the sensing, communication, processing, image acquisition, actuation, and power subsystems into a three-level modular structure.

During functional testing, the integration of the environmental and inertial sensors and their connection to the platform's acquisition and processing stages were verified. Figure 7 shows the integration and testing of the MQ-135, MQ-131, MLX90614, and BME280 sensors on the developed circuit board.

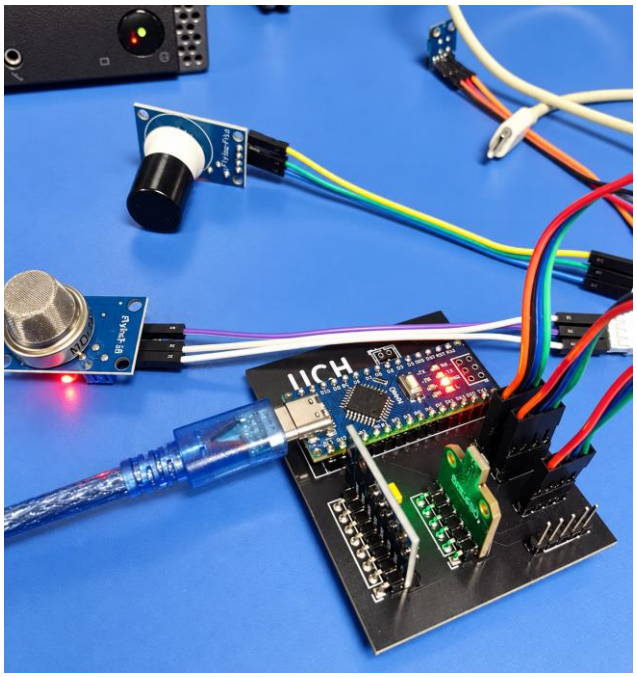

Fig. 7 Integration and testing of MQ-135, MQ-131, MLX90614, and BME280 sensors on a PCB.

Subsequently, the three subsystems were integrated into the mechanical structure of the UCH-SAT 3U. The use of modular design allowed keeping functional subsystems established during the design process separated and room created for on-board computer, sensors, communication parts and actuating system. There is a prototype, which was used for functional testing, presented on the Figure 8.

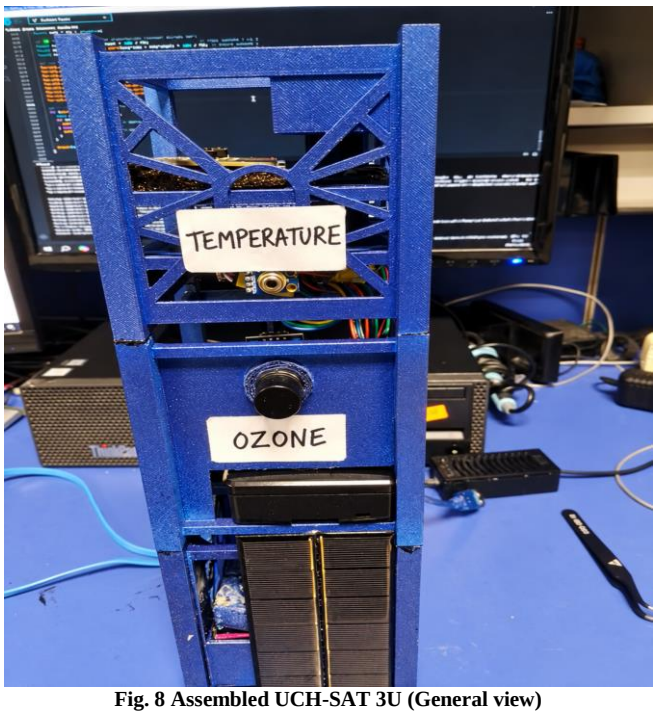

Fig. 8 Assembled UCH-SAT 3U (General view)

3.1.2. Graphical Interface and System Monitoring

A graphical interface was created to accompany the physical platform and provide a means of monitoring major subsystems of the UCH-SAT. The interface aggregated data from various sensors, the orientation of the vehicle, image acquisition, and the status of different subsystems. This integration facilitated the visual interpretation of the platform's overall performance and allowed for the organized display of system variables.

A camera view was incorporated at the top of the interface, allowing users to view the images captured by the system and providing controls to start or stop recording. Moreover, the diagrams for substations and the status of the solar panel operation were depicted, which enables users to visualize their activities during energy collection and storage. This enables users to associate the physical state of the platform and the control processes performed on the UCH-SAT.

Inertial data was also integrated by displaying the orientation obtained from the Inertial Measurement Unit (IMU). The interface shows the values for roll, pitch, and yaw, allowing users to observe changes in the platform's orientation. This feature complements sensor monitoring and facilitates the interpretation of the system's motion within the test environment. Also, graphical representations of the distinct environmental parameters from the system is displayed in the interface, such as presence of gas measured by the MQ-135, the ozone concentration as measured by the MQ-131, the temperature measured by the MLX90614 sensor in the infrared spectrum, the barometric pressure and altitude measured by the MS5611 sensor, as well as the values for relative humidity.

In addition, the interface indicates the quantity of active substations and the messages connected to the states of modules, making it possible to verify the presence of the components of the platform visually. Taken together, these features made the interface a key component of the UCH-SAT 3U, as it enabled the integration of sensor monitoring, orientation, image acquisition, recording, actuation, and overall system status into a single environment. The test shown in Figure 9 verified the organization and simultaneous display of these functions using the variables employed during the evaluation phase.

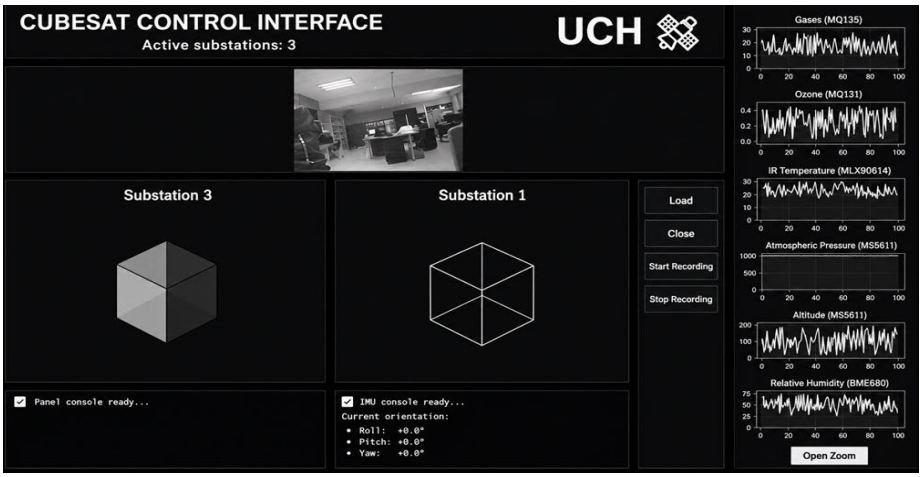

Fig. 9 Graphical interface test with simulated data

3.1.3. Photovoltaic Generation and MPPT Performance

The photovoltaic model was evaluated for irradiance levels of 400, 600, 800, and 1000 W/m². As shown in Figure 10(a), an increase in irradiance resulted in an increase in the current available in the photovoltaic array, while the open-circuit voltage exhibited a comparatively smaller change.

Figure 10(b) shows the corresponding effect on power, revealing a progressive increase in the maximum available power as irradiance increases.

These results made it possible to verify the response of the photovoltaic model before incorporating the maximum power point tracking algorithm.

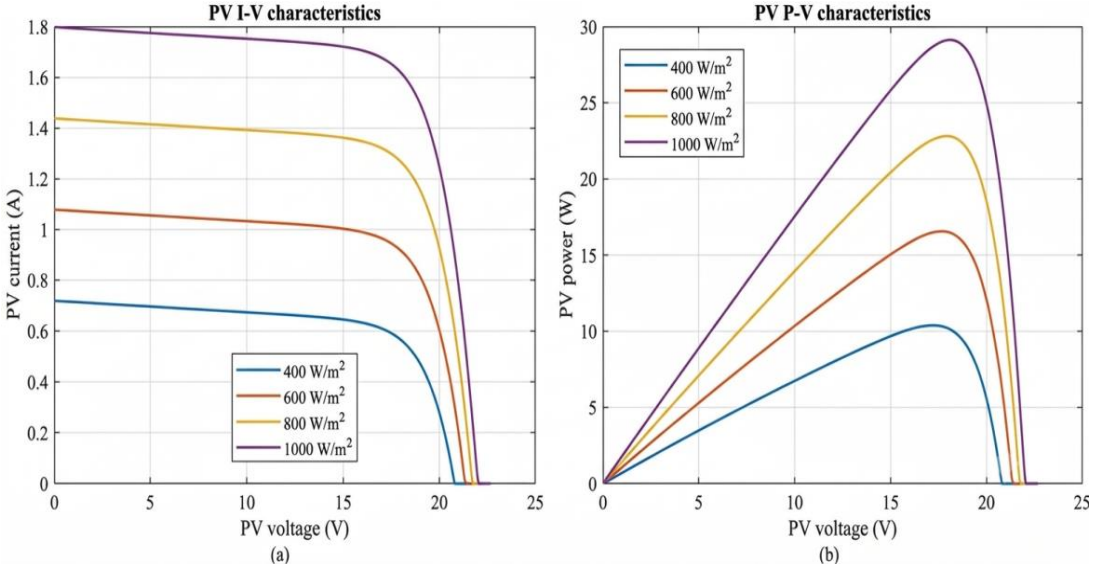

Fig. 10 Photovoltaic model response under different irradiance levels: (a) I-V characteristics, and (b) P-V characteristics.

The MPPT algorithm's response to temporal variations in irradiance was then evaluated. The applied profile produced successive changes in the maximum available power point, in response to which the tracked power closely followed the reference power, as shown in Figure 11.

For the evaluated interval, an MPPT tracking efficiency of 99.94% was obtained. The photovoltaic voltage exhibited small oscillations around the reference value associated with the disturbance-and-observation procedure.

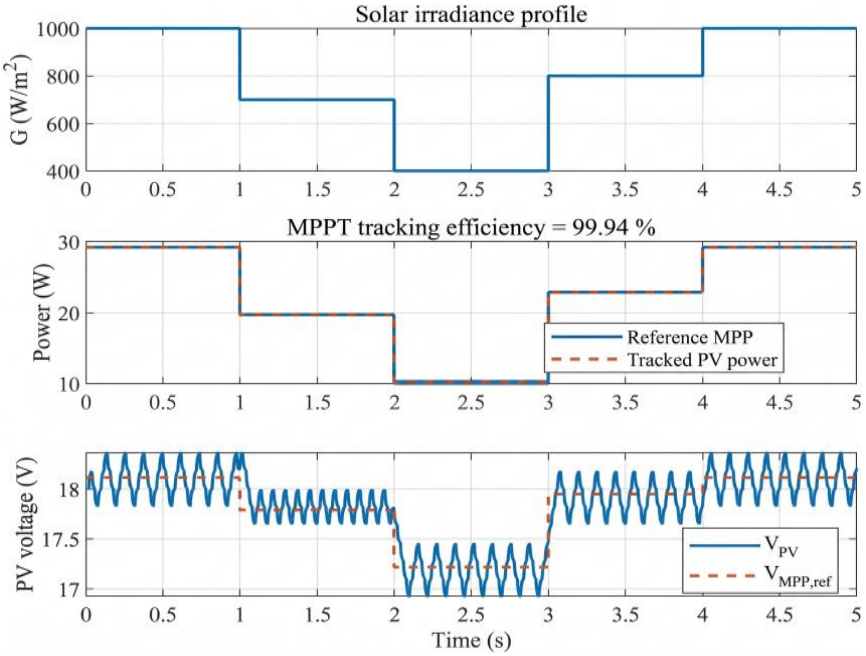

Fig. 11 MPPT tracking response under variable solar irradiance

3.1.4. EPS Transient Response and Storage Comparison

To analyze the dynamic response of the energy model, the same load change was applied to two storage configurations. When using the battery-only mode, the battery absorbed the demand fluctuations directly. This resulted in a minimum bus voltage of 14.122 V and the maximum current of 1.831 A drawn from the battery. The regulated outputs remained stable at 3.3V, 5V, and 12V despite the transients in the DC bus. At the same time, in the hybrid mode, the supercapacitor was used during the rapid demand change, decreasing the battery current. In this case, the bus minimum voltage was equal to 14.400V and the battery maximum current was equal to 0.946 A. In the discussed case of supercapacitor use, there was a reduction of approximately 48.3% in the maximum current drawn from the battery when compared with battery-only mode. Figure 12 gives the time comparison of the DC bus performance including regulated outputs and storage currents for both modes.

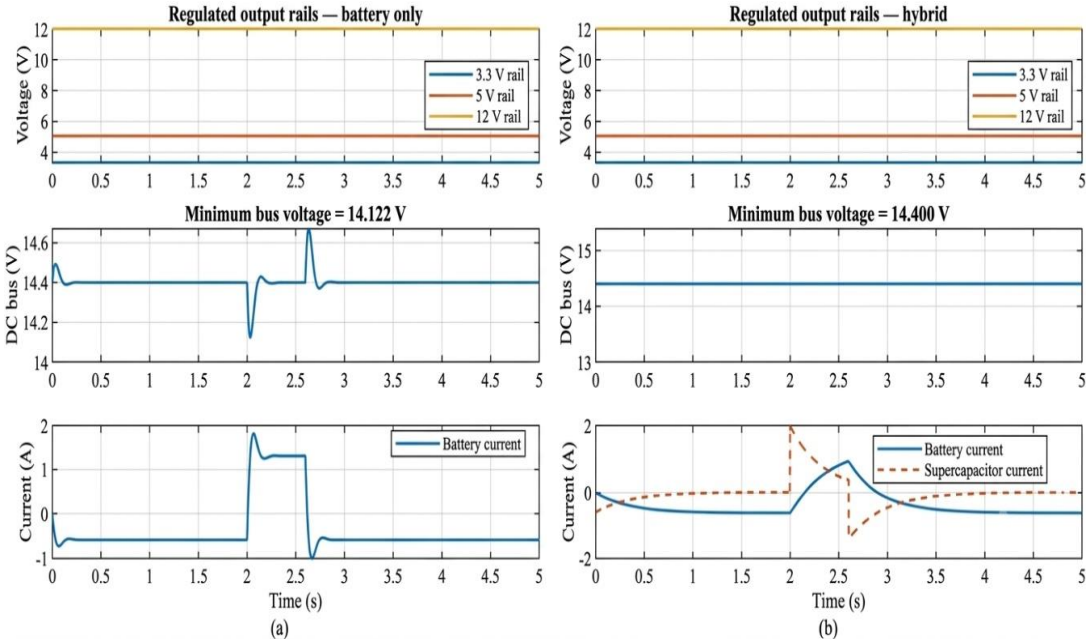

Fig. 12 EPS transient response under load variations: (a) Battery-only storage, and (b) Hybrid battery-supercapacitor storage.

3.2. Discussions

The results show that the modular architecture adopted for the UCH-SAT 3U made it possible to integrate sensing, communication, processing, and image acquisition functions onto a single platform. This approach is consistent with previous proposals that highlight modularity as a strategy for distributing the various subsystems and efficiently utilizing the available volume on CubeSat platforms [11, 12].

In the UCH-SAT, the division into three subsystems allowed for the functional separation of the modules and facilitated their integration within a 3U structure. Unlike proposals geared toward operational missions, the decision was made to focus on developing an educational architecture in which each subsystem can be monitored independently.

The use of sensors, microcontrollers, and Commercial off-the-Shelf (COTS) modules is also consistent with approaches reported for academic CubeSats. Garcia-Fernandez et al. [15] integrated commercial sensors, processing, and power management into a 1U experimental platform, while Sethi et al. [16] demonstrated the feasibility of using COTS components in power and communication subsystems. In the UCH-SAT 3U, this strategy made it possible to integrate environmental and inertial sensors, communication modules, an onboard computer, and actuators without requiring specialized components for space applications. However, the results pertain to an educational and experimental platform and therefore do not constitute a validation of performance under orbital conditions.

The importance of the graphical interface lies in the fact that it allows to display the environmental parameters such as orientation data obtained from IMU, image transmission, recording controls and the state in terms of the solar panels' deployment, all in one place. This advantage adds to the educational nature of the platform due to the fact that it allows relating the subsystems' operation to its visual representation.

This opinion is supported by research that use CubeSat projects in teaching engineering and technology courses [9] as well as by the projects indicating the necessity of applying systematic procedures in educational missions [10]. However, this study did not evaluate user learning quantitatively, hence the educational value is limited to the development of the platform and its monitoring system.

In the energy sector, the photovoltaic model was able to replicate the rise in both current and power as irradiance increased from 400 W/m² to its highest value of 1000 W/m². After this, the MPPT algorithm was able to track the change in maximum power point as a result of the changes in irradiance, with the efficiency being 99.94%.

This shows the importance of maximum power point tracking in the EPS settings in CubeSats where the efficiency of energy utilization is very important due to con [6, 18]. Nevertheless, the obtained efficiency result is only applicable to the specific simulation conditions since it refers to the modelling results rather than experimental efficiency of the physical MPPT converter.

The evaluation of storage methods indicated the most significant differences in case of temporary load variations. In a configuration containing a battery only, the lowest voltage level was equal to 14.122 V and the highest battery current was registered at 1.831 A.

In a design that included a supercapacitor, the minimum bus voltage was equal to 14.400 V, while the maximum current was reduced to 0.946 A, which suggests a reduction of approximately 48.3% in the considered scenarios. In both configurations, values of 3.3 V, 5 V, and 12 V were managed properly in terms of output. These findings show that the hybrid storage had a chance to handle the transient load and limit the current flowing from the battery. This requirement calls for having a comprehensive approach to power generation, storage, regulation, and distribution while developing EPS [6, 17].

Thanks to computational modeling, it became possible to make a provision of physical power system basis integrated in the UCH-SAT. Casado and his colleagues [17] used hardware-in-loop and simulation methods for evaluating CubeSat EPS architecture and proved the significance of computational modeling results in studying power flows and performance even before the introduction of the required system.

The model provided the possibility of an analysis of solar radiation, tracking of maximum power point, investigation of the reaction of DC bus and performance of the storage system without the real creation of advanced EPS structure. The key difference consists in the fact that the created model is aimed at the development of a 3U education platform and does not provide an experiment-based digital twin of the power system yet.

Overall, the results show that the UCH-SAT 3U can be used as a physical platform to study the interaction between sensors, communications, processing, image acquisition, and actuation, while the EPS computational model extends the analysis to phenomena related to energy generation and management.

This separation clearly distinguishes the results obtained from the prototype from those generated through simulation. The main limitation of the study is that the advanced EPS architecture was not physically implemented; therefore, the results related to MPPT, the DC bus, hybrid storage, and regulation require future experimental validation.

4. Conclusion

This project successfully developed UCH-SAT 3U, a modular educational platform consisting of three subsystems and an onboard computer. It integrates inertial and environmental sensing, communication, processing, image acquisition, actuation, and power supply functions. The graphical interface complements the platform by centralizing the display of essential variables, system orientation, substation statuses, image acquisition, and functions related to the deployment of the solar panels; it provides a monitoring and interaction environment for conducting tests and analyzing the system’s behavior.

As a complement to the physical platform, the EPS computational model allows for the simulation of photovoltaic generation, maximum power point tracking, the dynamic behavior of the DC bus, and various storage strategies. Under the simulated conditions, the MPPT algorithm achieves a tracking efficiency of 99.94%. Compared to a simple battery configuration, the hybrid battery-supercapacitor configuration maintains a minimum bus voltage of 14,400 V and reduces the peak battery current from 1,831 A to 0,946 A, representing an approximate reduction of 48.3%. Furthermore, the 3.3 V, 5 V, and 12 V output voltages are maintained. The combination of hardware, software, and a mathematical model results in a complementary approach for the functional implementation of the UCH-SAT 3U device's energy behavior. The experimental results obtained using the prototype and those derived from the simulation differ, preventing physical verification of the EPS program. Future work will focus on realizing an advanced EPS architecture, which will need to be implemented in hardware, and on experimentally verifying the simulation results, as well as incorporating the influence of temperature and other aspects typical of the space industry.

References

[1] Angela Cratere et al., “On-Board Computer for CubeSats: State-of-the-Art and Future Trends,” *IEEE Access*, vol. 12, pp. 99537-99569, 2024. [CrossRef] [Google Scholar] [Publisher Link]

[2] National Aeronautics and Space Administration (NASA), CubeSat Launch Initiative-Introduction, 2024, [Online]. Available: https://www.nasa.gov/cubesat-launch-initiative-introduction/

[3] Jasper Bouwmeester, Martin Langer, and Eberhard Gill, "Survey on the Implementation and Reliability of CubeSat Electrical Bus Interfaces," *CEAS Space Journal*, vol. 9, no. 2, pp. 163-173, 2017. [CrossRef] [Google Scholar] [Publisher Link]

[4] Varsha Parthasarath, and Philip Ferguson, "Modelling and Simulation of the Power Subsystem of a Low Earth Orbit CubeSat," *Aerospace Systems*, vol. 3, no. 2, pp. 139-146, 2020. [CrossRef] [Google Scholar] [Publisher Link]

[5] Andreas Johann Hörmer, Manuela Wenger, and Reinhard Zeif, "An Innovative FDIR Approach for the Power Supply of the PRETTY SDR Satellite Payload," *e and i Electrical Engineering and Information Technology*, vol. 139, no. 1, pp. 33-40, 2022. [CrossRef] [Google Scholar] [Publisher Link]

[6] Amarendra Edpuganti et al., "A Comprehensive Review on CubeSat Electrical Power System Architectures," *IEEE Transactions on Power Electronics*, vol. 37, no. 3, pp. 3161-3177, 2022. [CrossRef] [Google Scholar] [Publisher Link]

[7] National Commission for Aerospace Research and Development, CubeSats Project in Peru: From the Classroom to Space, Government of Peru, 2023. [Online]. Available: https://www.gob.pe/institucion/conida/noticias/828757-proyecto-cubesats-in-peru-de-las-aulas-al-espacio

[8] Agencia Andina, UNI Aims to put the Peruvian Modular Nanosatellite Chasqui 2 Into Orbit in 2026, 2024. [Online]. Available: https://www.radioaltamar.com.pe/uni-busca-poner-en-orbita-el-nanosatelite-modular-peruano-chasqui-2-en-2026

[9] Jesper A. Larsen, and Jens D. Nielsen, "Development of CubeSats in an Educational Context," *Proceedings of 5th International Conference on Recent Advances in Space Technologies-RAST2011*, Istanbul, Turkey, pp. 777-782, 2011. [CrossRef] [Google Scholar] [Publisher Link]

[10] Stephan Busch et al., "Robust Satelzlite Engineering in Educational CubeSat Missions at the Example of the UWE-3 Project," *IFAC Proceedings Volumes*, vol. 46, no. 19, pp. 236-241, 2013. [CrossRef] [Google Scholar] [Publisher Link]

[11] J. Bouwmeester, A. Menicucci, and E.K.A. Gill, "Improving CubeSat Reliability: Subsystem Redundancy or Improved Testing?," *Reliability Engineering and System Safety*, vol. 220, pp. 1-18, 2022. [CrossRef] [Google Scholar] [Publisher Link]

[12] Mohammad Suhel Karkun et al., "3U CubeSat Mechanical Design and Subsystems," *Acta Polytechnica*, vol. 65, no. 1, pp. 40-49, 2025. [CrossRef] [Google Scholar] [Publisher Link]

[13] Haythem Hussein Abdullah et al., "An Improved S-Band CubeSat Communication Subsystem Design and Implementation," *IEEE Access*, vol. 9, pp. 45123-45136, 2021. [CrossRef] [Google Scholar] [Publisher Link]

[14] Vahid Rastinasab, and Hu Weidong, "Implementation and Design of RF-Front-End Telemetry Tracking and Command Subsystem of a CubeSat with 500-km Altitude," *IEEE Journal on Miniaturization for Air and Space Systems*, vol. 2, no. 1, pp. 43-47, 2021. [CrossRef] [Google Scholar] [Publisher Link]

[15] Jose Pablo Garcia-Fernandez et al., "Measuring and Energizing Sensor System for Digital Signal Monitoring of an Academic-Experimental CubeSat for Wireless Telemetry Purposes," *Sensors*, vol. 23, no. 19, pp. 1-22, 2023. [CrossRef] [Google Scholar] [Publisher Link]

[16] Alakh Sethi et al., "Implementation of COTS Components for CubeSat Applications," *2017 IEEE Aerospace Conference*, Big Sky, MT, USA, pp. 1-11, 2017. [CrossRef] [Google Scholar] [Publisher Link]

[17] Pablo Casado et al., "Implementation of a 6U CubeSat Electrical Power System Digital Twin," *Aerospace*, vol. 11, no. 8, pp. 1-15, 2024. [CrossRef] [Google Scholar] [Publisher Link]

[18] Amarendra Edpuganti et al., "Comparison of Peak Power Tracking based Electric Power System Architectures for CubeSats," *IEEE Transactions on Industry Applications*, vol. 57, no. 3, pp. 2758-2768, 2021. [CrossRef] [Google Scholar] [Publisher Link]

[19] Mohamed El Bakkali et al., "Fully Integrated High Gain S-Band Triangular Slot Antenna for CubeSat Communications," *Electronics*, vol. 10, no. 2, pp. 1-26, 2021. [CrossRef] [Google Scholar] [Publisher Link]

[20] Ken Peffers et al., "A design Science Research Methodology for Information Systems Research," *Journal of Management Information Systems*, vol. 24, no. 3, pp. 45-77, 2007. [CrossRef] [Google Scholar] [Publisher Link]